Tumor-specific inhibitory action of decorin on different hepatoma cell lines.

Zsolt Horváth[1], Andrea Reszegi[1], László Szilák[2], Titanilla Dankó[1], Ilona Kovalszky[1], Kornélia Baghy[1]*

[1]1st Department of Pathology and Experimental Cancer Research, Semmelweis University, Budapest, Hungary

[2] Szilák Laboratories, Bioinformatics & Molecule-design Ltd. Szeged, Hungary

*Corresponding author

Address: 1st Department of Pathology and Experimental Cancer Research, Semmelweis University, Üllői street 26, Budapest, Hungary, H1085

email: baghy.kornelia@med.semmelweis-univ.hu; bcory6@gmail.com

Telephone: +36 1 459 1500 ext 54449

Fax: +36 1 317 1074

Running title: Tumor-specific inhibitory action of decorin in hepatoma cell lines

E-mail addresses for all authors:

Zsolt Horváth: hzsolt@korb1.sote.hu

Andrea Reszegi: areszegi2@gmail.com

László Szilák: laszlo.szilak@gmail.com

Titanilla Dankó: danko.titanilla@med.semmelweis-univ.hu

Ilona Kovalszky: koval@korb1.sote.hu

Kornélia Baghy: baghy.kornelia@med.semmelweis-univ.hu; bcory6@gmail.com

Highlights

- Decorin has an inhibitory effect on hepatoma cell lines without respect to their phenotype and molecular background
- Decorin is able to block the cell cycle at G2/M phase via phosphorylation of CDK1
- In p53 mutant hepatoma cell lines decorin compromises the activity of InsR and IGF-1R
- In hepatoma cell lines decorin modulates the activity of main signaling proteins such as AKT, ERK1/2 and β-catenin
- Decorin inhibits the production of TGF-β1 by tumor cells

Abstract

Background: In spite of therapeutic approaches, liver cancer is still one of the deadliest type of tumor in which tumor microenvironment may play an active role in the outcome of the disease. Decorin, a small leucine-rich proteoglycan is not only responsible for assembly and maintenance of the integrity of the extracellular matrix, but a natural inhibitor of cell surface receptors, thus it exerts antitumorigenic effects. Here we addressed the question whether this effect of decorin is independent of the tumor phenotypes including differentiation, proliferation and invasion.

Method: Four hepatoma cell lines HepG2, Hep3B, HuH7 and HLE, possessing different molecular backgrounds, were selected to investigate. After proliferation tests, pRTK arrays, WB analyses, and immunofluorescent examinations were performed on decorin treated and control cells for comparison.

Results: Significant growth inhibitory potential of decorin on three out of four hepatoma cell lines was proven, however the mode of its action was different. Induction of $p21^{WAF1/CIP1}$, increased inactivation of c-myc and β-catenin, and decrease of EGFR, GSK3β and ERK1/2 phosphorylation levels were observed in HepG2 cells, pathways already well-described in literature. However, in the p53 deficient Hep3B and HuH7, InsR and IGF-1R were the main receptors transmitting signals. In harmony with its receptor status, Hep3B cells displayed high level of activated AKT. As the cell line is retinoblastoma mutant, ATR/Chk1/Wee1 system might hinder the cell cycle in G2/M phase via phosphorylation of CDK1. In Huh7 cells, all RTKs were inhibited by decorin followed by downregulation of AKT. Furthermore, HuH7 cell line responded with concentration-dependent ERK activation and increased phospho-c-myc level. Decorin had only a non-significant effect on the proliferation rate of HLE cell line. However, it responded with a significant decrease of pAKT, c-myc and β-catenin activity. In

this special cell line, the inhibition of TGFβ may be the first step of the protective effect of decorin.

Conclusions: Based on our results decorin may be a candidate therapeutic agent in the battle against liver cancer, but several questions need to be answered. It is certain that decorin is capable to exert its suppressor effect in hepatoma cells without respect to their phenotype and molecular background.

Keywords

decorin, hepatoma cell line, liver carcinoma, tumor-specific inhibition, proliferation inhibition

1. Introduction

Hepatocellular carcinomas (HCC), representing the vast majority of the primary liver cancers, are the second leader cause of death among malignant tumors worldwide (782,000 cases and 745,000 deaths annually) [1]. The development of HCC depends on multiple factors, such as etiology and/or severity of other underlying diseases, lifestyle of patients, behavioral and environmental risk factors [2]. Influenced by these circumstances, HCC progression is a complex process which involves several molecular regulatory pathways of hepatoma cells, and the actual conditions of the tumor microenvironment. In most of the cases human HCCs develop from cirrhotic liver. Within years chronic inflammation and hepatocyte regeneration, together with the oncogenic action of hepatitis viruses and action of inflammatory cytokines push cirrhotic liver toward the development of liver cancer [3].

TGF-β is one of the major profibrotic cytokines involved in development of liver cirrhosis by stimulating nonparenchymal liver cells, especially hepatic stellate cells, and portal fibroblasts, for synthesis of excess extracellular matrix (ECM) [4]. Increasing amount of ECM

in cirrhosis results in elevated levels of connective tissue proteins and proteoglycans, including decorin.

Decorin is a small leucine rich proteoglycan (SLRP), which as a member of extracellular matrix is responsible for maintaining the structural integrity of collagens [5]. Decorin binds to collagens, therefore has a spacer function between matrix fibers ensured by its glycosaminoglycan (GAG) side chain. It can be found in a variety of connective tissues, including skin, tendon, cartilage, and bone. In the healthy liver, the amount of decorin is quite low, its interstitial deposition is correlated with the increase of other connective tissue elements during fibrogenesis [6, 7].

Researches of the past decades show that decorin has an inhibitory effect on tumor progression. Overexpression of decorin inhibits the proliferation of colorectal cancer cells [8], ovarium carcinoma cells [9] and breast cancer cells [10] in vitro. Furthermore, it prevents tumor cell-mediated angiogenesis [11] and effectively blocks metastatic spreading of breast cancer [12]. Several studies hypothesize that decorin may have a role in tumorigenesis of various other organs such as pancreas [13] or larynx [14] and these are only a few examples out many data, reported in recent years. Decorin was reported to suppress proliferation of HepG2 hepatoma cell line through $p21^{WAF1/CIP1}$ upregulation [15], and our previous investigations showed that decorin deficiency promotes hepatic carcinogenesis in vivo [16].

The best known mechanism of decorin antiproliferative action is its capability to bind to and inhibit cell surface tyrosine kinase receptors. Decorin core protein effectively binds to EGFR [17], IGF-IR [18], ErbB2 [19], Met (HGF receptor) [20] and VEGFR-2 [21]. Furthermore, decorin can interact with the natural ligand PDGF rather than to the receptor itself hindering downstream signaling pathways [22]. Decorin is also able to bind and inhibit TGF-β1, which leads to attenuated connective tissue production and hindered fibrogenesis [23]. Via these interactions decorin can prevent the binding of a particular ligand to its receptor, it can

activate the receptors similarly to their ligands, and/or can cause caveolin-mediated receptor internalization [24]. Howsoever it happens; decorin binding provokes intracellular signals which has an impact on cell proliferation [25-27].

When surgical removal cannot be taken into account, the management of hepatocellular cancer is not resolved. Therefore, better understanding of the molecular mechanisms driving HCC progression together with seeking for new approaches in its treatment has an urging importance.

Accordingly, by using recombinant decorin, we focused our research on human hepatoma cell lines HepG2, Hep3B, HuH7 and HLE to gain more information about the mechanism as this proteoglycan hinders their progression. We addressed the question if decorin has the potential to inhibit the proliferation of these hepatoma cell lines without respect of their phenotype. Furthermore, we aimed to explore the underlying molecular mechanisms leading to the observed effects of decorin.

2. Material and methods

2.1. Production of human recombinant decorin

For proteoglycan production a pCMV expression vector (Thermo Fisher Scientific, Waltham, MA, USA) construct containing the human decorin cDNA sequence was created (Szilák Laboratories, Bioinformatics & Molecule-design Ltd. Szeged, Hungary). Next, CHO-S (Chinese hamster ovary) cells (Gibco/Thermo Fisher) were transfected by the expression vector using electroporation by Neon™ transfection system, following manufacturer's recommendations (Invitrogen/Thermo Fisher). Successfully transfected cells were selected by adding 500 μg/ml of G418 solution to cell culture medium (Sigma) and human recombinant decorin production was conducted following manufacturer's recommendations (Gibco/Thermo Fisher). The recombinant proteoglycan was isolated as previously described [28]. After chromatographic purification the samples were dialyzed against distilled water and the

proteoglycan content was checked by dimethyl methylene blue (DMB, Sigma-Aldrich, St. Luis, MO, USA) staining. Finally, salts were added to the samples to convert the distilled water to 1x phosphate buffered saline (PBS), and the final decorin concentration was adjusted to 1000 μg/ml. These stock solutions were stored at -20˚C until use.

2.2. Tissue culture and reagents

HepG2 and Hep3B cell lines were obtained from the American Type Culture Collection (Manassas, VA, USA), HuH-7 and HLE were acquired from the Japanese Collection of Research Bioresources Cell Bank (Osaka, JP). Cells were cultured in Dulbecco's modified Eagle's medium (Sigma-Aldrich, St. Luis, MO, USA) with 1000 mg/L (5.5 mmol/l) glucose concentration, supplemented with 10% [v/v] fetal bovine serum (Sigma), and 1% [v/v] (Penicillin/Streptomycin (Sigma) in an atmosphere containing 5% CO_2 at 37 °C. Decorin was dissolved in sterile PBS and added to culture medium at final concentrations of 50 or 100 μg/ml (DCN50 and DCN100 groups) after 24 hours of serum deprivation. Cultivation of cells is detailed in the particular assays.

2.3. Proliferation assay

Cell proliferation was estimated using a 3-(4,5-dimethylthiazol-2-yl)-2, 5-diphenyl tetrazolium bromide (MTT) assay (Sigma) measuring metabolic activity. Cells were plated in 96-well flat bottom tissue culture plate, containing 100 μl of DMEM (supplemented with 10% FBS) tissue culture medium, at a concentration of 2×10^3 cells/well for HepG2 and HLE, and of 5×10^3 for Hep3B and HuH7 hepatoma cell lines. After adhesion of cells, medium was changed to serum free DMEM for 24 h. The experiment was performed in serum deprived conditions for 0, 24, 48 and 72 h at 0, 50 and 100 μg/ml decorin concentration. Each well contained 180 μl medium and additional 20 μl PBS with the appropriate amount of decorin.

Twenty µl MTT solution was added per well at the endpoints. After 4 h incubation, formazan crystals were dissolved in 150 µl of DMSO. Plates were shaken for 1 min and optical density was read on a multi-well scanning spectrophotometer (Labsystems Multiskan MS) at 570 nm.

2.4. Enzyme-linked immunosorbent assay (ELISA)

TGF-β1 content in culture medium was assessed using Solid Phase Sandwich ELISA kit (Quantikine R&D Systems, Minneapolis, MN, USA, Cat. No.: DB100B). Fifty µl of medium was added to the microplate wells, and each sample was tested in triplicates. The procedure was performed according to the manufacturer's recommendation.

2.5. Phospho-RTK array and Western blot

Cells grown in T25 cell culture flasks were harvested at 15 min and 48 h time points by using 1.0 ml lysis buffer (20 mM TRIS pH 7.5, 2 mM EDTA, 150 mM NaCl, 1% Triton-X100, 0.5% Protease Inhibitor Cocktail (Sigma) 2 mM Na_3VO_4, 10 mM NaF). After sonication and incubation for 30 min on ice, samples were centrifuged at 15,000 g for 5 min. Supernatants were kept and protein concentrations were measured by Bradford protein assay (Bio-Rad Laboratories, Hercules, CA, USA). The activities of phospho-receptor tyrosine kinases (Phospho-RTKs) were assessed by their relative levels of phosphorylation using the Proteome Profiler Human Phospho-RTK Array Kit (Cat. no.: ARY001B, R&D Systems, Minneapolis, MN, USA) according to the manufacturer's instructions. Two hundred µg of total proteins was added to each membrane. Signals were developed by incubating the membrane in SuperSignal West Pico Chemiluminescent Substrate Kit (Pierce/Thermo Fisher Scientific, Waltham, MA, USA), and visualized on a Kodak Image Station 4000MM Digital Imaging System.

For Western blot, 20 µg of total proteins were mixed with loading buffer containing 1.5 v/v% β-mercaptoethanol and incubated at 99 °C for 5 min. Denatured samples were loaded onto

a 10% polyacrylamide gel and were run for 30 min at 200 V on a Mini Protean vertical electrophoresis equipment (Bio-Rad). Proteins were transferred to a PVDF membrane (Millipore, Billerica, MA, USA) by blotting for 16 h at 75 mA. Ponceau staining was applied to determine blotting efficiency. Membranes were blocked with 5 w/v% non-fat dry milk (Bio-Rad) in TBS for 1 h followed by incubation with the primary antibodies at 4 °C for 16 h. Beta-actin immunostaining served as loading control. Membranes were washed 5 times with TBS containing 0.05 v/v% Tween-20, then were incubated with appropriate secondary antibodies for 1 h. Signals were detected by SuperSignal West Pico Chemiluminescent Substrate Kit (Pierce/Thermo Fisher Scientific) and visualized by Kodak Image Station 4000MM Digital Imaging System. Western blot analyses were performed 3 independent times. The density of the bands was measured by the Kodak Image Station. For antibody specifications and dilutions applied see Supplementary Table 1.

2.6. Immunocytochemistry

Cells were cultured in 6-well plates (with seeding density of 1.3×10^5 cells/well for HepG2 and HLE, and 2.15×10^5 cells/well for Hep3B and HuH7), each well contained a sterilized glass coverslip. After 24 hours of serum starvation the cells were exposed to decorin for 48 hours (in the same conditions as it was previously described). Cells were fixed in ice-cold methanol for 10 min. Coverslips were washed with phosphate buffered saline with 0.05% Tween 20 (PBST), and aspecific binding sites were blocked with 5% bovine serum albumin (BSA) dissolved in PBS. Cells were incubated overnight at 4°C with primary antibody (anti-CTNNB1; HPA029159; Sigma) at a dilution of 1:100. Thereafter, cells were washed and incubated with secondary antibody (AlexaFluor 488; Invitrogen/Thermo Fisher Scientific) and DAPI for one hour. After the last washing procedure, fluorescent mounting media (Dako,

Glostrup, Denmark) was applied, and epifluorescent microscope (Nikon Eclipse E600) was used for evaluation.

2.7. Statistical analysis

All statistical analyses were performed using GraphPad Prism 7.00 software (Graphpad Software Inc., La Jolla, CA, USA). Data were tested for normal distribution using the omnibus normality test of D'Agostino & Pearson. Significance of changes were tested using a nonparametric test (the Mann–Whitney U-test) or the Student's t-test, depending on the distribution of the data. The independent experimental sets were compared for reproducibility. Only reproducible significant changes were considered as significant. Significance was declared at the standard $p < 0.05$ level.

3. Results

3.1. Proliferation inhibitory action of decorin is different in the hepatoma cell lines.

To capture the effect of decorin on cell proliferation MTT assay was performed on each cell line. As Figure 1. shows, proliferation rate of 3 out of 4 hepatoma cell lines were significantly inhibited upon decorin exposure.

The growth inhibition of Hep3B appeared 24 hours after decorin exposure and was sustained during the entire experiment. Similar effect was observed on HepG2 cells, however decreased efficiency of decorin was seen at 48 hours. The Huh7 cell line reacted to exogenous decorin only after 48 hours, but the inhibitory effect lasted until the end of the experiment. In contrast, HLE cells showed only a slight decrease in proliferation rate after 72 hours, but the difference did not reach statistical significance.

3.2. Decorin has an impact on TGF-β1 secretion

As TGF-β1 is a known binding partner of decorin, we studied the secreted amounts of the growth factor by ELISA from cell culture supernatants. Figure 2. shows the levels of TGF-β1 after a 48-hour exposure to 50 and 100 μg/ml decorin normalized to untreated controls. In HepG2 cell line, a significant decrease in the growth factor level was measured in DCN50 and DCN100 groups by 49% and 21% respectively ($p<0.05$). TGF-β1 secretion was significantly hindered in Hep3B (29% and 36% in DCN 50 and DCN100 groups in ($p<0.01$, $p<0.05$)) and HLE cells as well; 68% and 53% in treated groups ($p<0.05$). However, no significant change in secreted TGF-β1 amount was detected in HuH7cells upon decorin exposure.

3.3. Different signaling pathways are provoked by decorin in hepatoma cell lines

Next, we aimed to unravel the signaling processes provoked by decorin in each particular cell line. To this end, tyrosine kinase receptors and their major signaling pathways implicated in the proliferation of hepatomas (MAPK, WNT, PKB/Akt) has been studied. In addition, expression of representative proteins of cell cycle have been detected.

3.3.1. The "conventional" HepG2

After an early activation of EGFR receptor upon 15 min decorin treatment, (Fig. S1), EGFR was the only detectable phosphorylated RTK in HepG2 cells (Fig. 3) at the 48 h time-point. Its phosphorylation decreased upon decorin exposure in a dose dependent manner (Fig. 3). Cells exposed to 50 (DCN50) or 100 μg/mL (DCN100) decorin displayed a decrease of the receptor by 48% and 84% respectively relative to the control cell population ($p<0.001$, Fig. 3).

Decreased EGFR phosphorylation went parallel with reduced activation of ERK1 (30% in DCN50 and 22% in DCN100 groups relative to control [$p < 0.001$ and non-significant]), and ERK2 proteins (79% and 64% in DCN50 and DCN100 [$p<0.001$ in both groups]). Furthermore,

levels of the cyclin-dependent kinase inhibitor $p21^{WAF1/CIP1}$ and $p27^{KIP1}$ were elevated. We observed a 4.8-fold and a 3.7-fold increase in $p21^{WAF1/CIP1}$ protein in DCN50 and DCN100 groups respectively ($p<0.01$ in both groups). In case of $p27^{KIP1}$, a 1.74-fold and a 1.5-fold elevation was measured in DCN50 and DCN100 groups after 48 hours of treatment ($p<0.01$ and $p<0.05$) (Fig 4.). No considerable change in Akt phosphorylation was found.

Regarding to other signaling pathway proteins, we focused on the phosphorylation of c-myc, GSK3α/β and β-catenin (Fig 4.). In HepG2 cells, decorin exposure resulted in reduced phosphorylation of GSK3α/β, and elevated levels of phospho-β-catenin. Phosphorylation of GSK3α was decreased by 15% and 44% in DCN50 and DCN100 groups, relative to control ($p<0.05$ and $p<0.01$), while phospho-GSK3β amount was reduced by 39% and 50% ($p<0.001$ in both groups). As a result, we observed elevated phosphorylation of β-catenin (2.1-fold and 2.4-fold in DCN50 and DCN100 groups vs. control, $p<0.01$ in both groups), and c-myc (2.5-fold and 4.7-fold in DCN50 and DCN100 groups vs. control; $p<0.05$ and $p<0.01$) (Fig 4.).
In harmony with these results β-catenin vanished from the nuclei of HepG2 cells (Fig. 5) showing immunolocalization on the cell membrane after 48 hours of decorin treatment.

3.3.2. The "restriction point deficient" Hep3B

The Hep3B cell line bears a deleterious mutation in genes coding for p53 and retinoblastoma proteins resulting in failure in cell cycle blockade in G1 phase. Regarding TK receptors, changes in EGFR, InsR and IGF-IR phosphorylation were detected upon decorin exposure (Fig. 3). At 15 min, inhibition of EGFR by decorin was observed in Hep3B cells, and no change in InsR and IGF-1R levels were detected (Fig. S1). After 48 h, similarly to HepG2, the active EGFR level was reduced by 13% and 49% in DCN50 and DCN100 groups relative to control cells (non-significant in DCN50 and $p<0.01$ in DCN100); however we found enhanced activation of InsR and IGF-IR in Hep3B cells. While pInsR increased with 1.56-fold

in DCN50 group compared to untreated control ($p<0.05$), the elevation was not significant in DCN100 group. For pIGF-IR, the pattern was quite similar, 1.23-fold increase was detected in DCN50 vs. control ($p<0.05$), however the change in DCN100 group did not reach statistical significance (Fig. 3).

In parallel with IGF and insulin receptor activation we found considerable elevation in AKT level, phosphorylated on threonine 308 residue (Fig. 6.). A 10.8 and a 9.7-fold increase was observed in DCN50 and DCN100 groups compared to untreated control Hep3B cells ($p<0.01$ and $p<0.001$ respectively). While a 37% increase of pERK1 was detected in both treated populations; ($p<0.05$ in DCN50 group and non-significant in DCN100 group), we found no significant change in the phosphorylation of ERK2. We did not detect $p21^{WAF1/CIP1}$ in Hep3B cell line either in untreated, or in decorin exposed cells. However, the amount of $p27^{KIP1}$ protein was significantly increased after 48 hours of decorin exposure; 71% and 76% elevations were observed in DCN50 and DCN100 groups ($p<0.01$ and $p<0.001$). While phosphorylation of GSK3α showed no alternations after decorin treatment compared to the control cells, minor elevations were detected in case of phospho-GSK3β levels after treatment (26% and 12% in DCN50 and DCN100 groups; $p <0.05$ in both cases). We could not detect phospho-c-myc in Hep3B cells and there was no significant change in phospho-β-catenin levels (Fig. 6).

As Hep3B cells are TP53 and RB mutant, we needed to look for a cell cycle regulator beyond G1 phase. We found a marked induction of CDK1 phosphorylation in these cells. We observed 2.42-fold elevation in DCN50 group, and a 2.04-fold increase in DCN100 population ($p<0.01$ in both groups) (Fig. 7.). In parallel with the increased phospho-CDK1 level, a 24% decrease in phosphatase Cdc25A and a 35% elevation in Wee1 kinase mRNA level were detected in DCN50 group.

3.3.3. The "p53 mutant" HuH7

The HuH7 cell line carries a missense mutation in p53 gene resulting in the overexpression of the mutant protein with oncogenic properties. After 15 min, decorin was able to decrease the level of active EGFR, and induced InsR and IGF-1R phosphorylation. Minute amounts of active FGFR and RYK were also seen on the membranes (Fig. S1). After 48 h, the HuH7 cells displayed active EGFR, InsR and IGF-IR similarly to Hep3B. EGFR phosphorylation was significantly decreased after decorin exposure by 20% in DCN50 group and by 42% in DCN100 group ($p<0.05$ in both cases). InsR and IGF-IR phosphorylation were also altered, although we could not detect significant change in the DCN50 group of HuH7 cells. However, phospho-InsR level was decreased by 34% and IGF-1R phosphorylation was lessened by 28% in DCN100 group ($p<0.05$ in both cases, Fig. 3.).

Akt phosphorylation was extensively inhibited after 48 hours of decorin exposure in HuH7 cells. 44% loss of phosphorylated Akt was seen in DCN50, and 82% in DCN100 group ($p<0.001$ and $p<0.001$). In contrast to our previous findings, we detected massive ERK activation. A 2.8-fold and a 3.9-fold elevation were found in pERK1 levels in DCN50 and DCN100 groups relative to control cells ($p<0.001$ and $p<0.01$), while a 12.7-fold and a 19.8-fold increase was observed in case of ERK2 ($p<0.001$ in both cases).

We could not detect $p21^{WAF1/CIP1}$ in HuH7 cells. $P27^{KIP1}$ displayed no major alternation after decorin treatment. GSK3 phosphorylation displayed a very similar pattern to that of pInsR and pIGF-IR. Phospho-GSK3α level did not increase significantly in DCN50 group, while it lessened by 61% in DCN100 group ($p<0.01$). In parallel, phospho-GSK3β level elevated by 32% in DCN50 group, while it decreased by 62% in DCN100 group ($p<0.05$ and $p<0.001$) of HuH7 cells. We found intensive upregulation of c-myc phosphorylation after decorin exposure. A 3.17 and a 2.92-fold increase was detected in DCN50, and in DCN100 groups respectively, compared to the untreated control cells ($p<0.001$ and $p < 0.01$). We could not detect phosphorylated β-catenin in HuH7 cell line (Fig. 8.).

3.3.4. The "fibroblast-like" HLE

HLE cells share several features with mesenchymal cells such as the ability to migrate and being vimentin positive. After 15 min, active EGFR was detected in HLE cells, but the proteoglycan did not alter their levels. Trace amounts of RYK, ErB3 and Axl were also detected (Fig. S1). Interestingly, no phosphorylated RTK was detected in the cell line after 48 h. Despite of this, we found considerable downregulation of Akt phosphorylation, 66% and 64% decrease in DCN50 and DCN100 groups relative to the control population of HLE cells ($p<0.001$ in both cases). However, no major changes were observed in pERK1 and pERK2 levels. While the protein level of $p27^{KIP1}$ did not alter upon decorin exposure, the $p21^{WAF1/CIP1}$ amount showed significant upregulation (2.45 and 1.82-fold increase in DCN50 and DCN100 group, respectively; $p<0.05$ and $p<0.01$). The phospho-GSK3 protein levels slightly decreased. GSK3α phosphorylation lessened by 4% and 17% in decorin-exposed groups ($p<0.05$ in DCN100 group), while phospho-GSK3β decreased by 8% and 12% in DCN50 and DCN100 groups compared to untreated HLE cells ($p<0.05$ in DCN100 group). While phospho-c-myc amount showed no change at all in DCN50 group relative to control, we found a 37% increase in DCN100 group ($p<0.001$). Finally, considerable upregulation in β-catenin phosphorylation was observed in HLE cells; 2.8 and a 3.1-fold elevation in DCN50 and DCN100 groups were detected compared to control population ($p<0.05$ in both cases) (Fig. 9.). In parallel disappearance of the protein from the nucleus and the cytoplasm was also observed by immunostaining after decorin treatment (Fig. 5. C, D).

4. Discussion

Previously we proved the protective role of decorin against thioacetamide (TA) and diethylnitrosamine (DEN) induced hepatocarcinogenesis [16], however it was a further

question whether the proteoglycan shows efficacy against human hepatomas, as well. The question is all the more important, as management of liver cancers other than surgery fails to provide improvement for decades [29].

The inhibitory effect of human recombinant decorin on HepG2 cells through $p21^{WAF1/CIP1}$ [15] and $p57^{KIP2}$ upregulation was previously reported [30], therefore HepG2 was applied as an internal control in our experiments. Our results obtained on this cell line were in a full agreement with the literature data. Decorin exposure was able to diminish the proliferation rate of HepG2 cells, although its rate of inhibition slowed down at 48h. The other two differentiated hepatoma cell lines, Hep3B and Huh7, showed stepwise decrease in proliferation starting at 24 and 48 hours respectively. However, decorin did not inhibit the proliferation of HLE cells. Detailed analysis of signaling pathways revealed that decorin initiates different molecular responses in our hepatoma cell lines even if their antiproliferative response is identical. For HepG2 cells, activation of EGFR provides stimulus for continuous proliferation, and decorin initiates its effect through downregulation of EGFR signaling [31]. Accordingly, we observed a concentration-dependent inhibition of EGFR, with decreased phospho-ERK1/2, and elevated $p27^{KIP1}$ and $p21^{WAF1/CIP1}$ amounts in HepG2 cells. Furthermore, decrease in degradative phosphorylation of GSK3α/β was noticed which could be related to the signaling events described above, as downregulation of ERK1/2 activity can result in reactivation of GSK3β [32]. This leads to phosphorylation and subsequent proteasomal degradation of β-catenin and c-Myc [33]. As an effect of decorin the nuclear localization of β-catenin decreased, and the protein mainly localized in the cell membrane of HepG2 cells (Figure 10).

However, neither Hep3B, nor HuH7 cells use EGFR as primary signaling receptor. In contrast, basic activities of insulin receptor (InsR) and IGF-1R were inherently higher than that of EGFR in both cell lines. These activities increased further upon decorin exposure in Hep3B cell line, while they were hindered in case of HuH7. A common feature of these two cell lines

is that both of them harbor mutation in the TP53 tumor suppressor gene. Hep3B cells carry a homozygote deletion, while HuH7 cell line harbors the p.Y220C point mutation leading to overproduction of mutant protein, and oncogenic activity [34]. Research of the past years has highlighted that p53 plays a key role in regulation of metabolism. It influences glycolysis, mitochondrial oxidative phosphorylation, pentose phosphate pathway, fatty acid synthesis and oxidation, and maintenance of homeostasis. Participating in these processes contributes to the tumor suppressor function of the protein [35, 36]. Wild type p53 also inhibits the transcription of insulin receptor and IGF-1R [37], giving explanation for the high levels of these receptors in p53 mutant Hep3B and HuH7 cell lines. Furthermore, Hep3B and Huh7 produce large amount of insulin receptor substrates (IRSs), primarily IRS-2 [38].

In Hep3B cells, decorin exposure provoked activation both of InsR and IGF-IR followed by massive Akt, and a slight MAPK phosphorylation. This was previously shown in normal endothelial cells, renal fibroblasts and extravillous trophoblasts that decorin is capable of activating IGF-IR receptor and thus inducing Akt phosphorylation [24]. However, in tumor cells activation of IGF-IR and IR caused by decorin has not been observed yet. Since the Hep3B cell line is well-differentiated, it is conceivable, that depending on the extent of differentiation, decorin may activate IGFR as it was observed in normal cells, or it may inhibit the receptor, as it was found in other tumor cells [24]. Xiong et al. showed the supportive role of IGF-1R in p53-mediated apoptosis [39], while Yoon and his group reported that adenovirus-mediated decorin expression leads to cell death by activating p53 [40]. These two publications may indicate that decorin as part of the IGF-1R-p53 feed-back loop, try to compensate for the lack of p53 by upregulating the TK receptor. This theory may explain our observation, why we experienced IGF-1R activation in the p53 deleted Hep3B, and receptor inhibition in HuH7, where mutant p53 is highly expressed. Since beside p53 Hep3B is also retinoblastoma deletion mutant [41], cell cycle arrest at the restriction point G1/S is compromised, thus cells will

certainly cross the checkpoint. It is a known phenomenon that increased Akt activity may lead to hyper-replication ending up in replication stress that activates the ATR/Chk1/Wee1 system stopping the cell cycle in G2/M phase via phosphorylation of CDK1 [42]. Indeed, in Hep3B cells, the levels of pCDK1 and Wee1 increased in parallel with the high phospho-Akt levels, while expression of Cdc25A phosphatase decreased simultaneously, supporting the idea of the aforementioned mechanism. Our experiments clarified that decorin not only inhibits the G1/S phase transition, but also is capable to block the further step of the cell cycle from G2 to M phase (Figure 10.). This inhibitory effect of the proteoglycan has been completely unknown so far, therefore more studies are needed to reveal underlying signaling processes. However, this newly discovered impact of proteoglycan on G2/M cell cycle processes further reinforces the tumor suppressor ability of decorin.

In the HuH7 cell line, decorin administration reduced the amount of phospho-InsR and phospho-IGF-1R, as expected. In addition, we witnessed a concentration dependent decrease in the phosphorylation of EGFR after decorin exposure, similarly to that of HepG2 and Hep3B cells. In parallel with the inhibition of receptors, a dose-dependent lessening of pAkt amount was observed. As a consequence, the phosphorylation of GSK-3 decreased accompanied by elevated phospho-c-Myc level. Although we found no detectable change in levels of $p21^{WAF1/CIP1}$ or $p27^{KIP1}$, c-Myc deactivation might cause alternations in cell cycle regulation, such as induction of $p15^{INK4B}$ or$p16^{INK4A}$, or inhibition of Cyclin A2, Cyclin D2 and Cyclin E1, all are specific partner genes of c-Myc [43]. The most remarkable change, we observed in these experiments was the massive ERK activation (Figure 10). Similar phenomenon was described previously in HuH7 cell after cisplatin exposure [44]. This ERK phosphorylation ultimately leads to apoptosis, thus, activated ERK1/2 can act as tumor suppressor molecules in HuH7 cells [45]. Furthermore, it was proposed that ERK1/2 may initiate either stimulatory or inhibitory effect on proliferation and the level of its activity determines that which of the

opposite actions will prevail [46]. Additional investigations are needed to clarify the exact mechanisms of signal transduction after decorin treatment in HuH7 hepatoma cell line.

Among the investigated HCC cell lines HLE is considered as a non-differentiated one [47], as supported by its strong vimentin positivity. This might be the reason why we could not find any activated EGFR even on the surface of untreated control cells. Furthermore, neither of the examined RTKs was active in HLE cells. In harmony with that HLE cells showed no considerable change in ERK1/2 phosphorylation. In the light of this, it becomes more understandable, that we found only a minor suppression of cell proliferation by MTT assay. On the other hand, 48 hours after decorin exposure, more than 50% decrease of TGFβ1 was observed together with significant downregulation of $pAkt^{Thr308}$ [48]. As HLE already went through the process of EMT [49], where Akt activation plays crucial role, we may say that in this case decorin interferes with EMT, and exerts modest antiproliferative action. The slight GSK3β activation which could explain the inactivating phosphorylation of β-catenin and c-Myc (Figure 10.) with subsequent $p21^{WAF1/CIP1}$ induction were insufficient to block or slow down the proliferation rate of HLE cells after 72 hours of decorin exposure. Since many mesenchymal cells can internalize the decorin [50, 51], it is conceivable that mesenchymal–type HLE also possesses a decorin-specific endocytosis receptor.

Further evidence for the mesenchymal behavior of HLE cells is their ability to migrate, which is enhanced by TGFβ treatment [52]. On the other hand, Dzieran and coworkers described, that HLE cell line is insensitive to the cytostatic effect of growth factor, which can explain the result of our MTT assay. The bipolar behavior of TGFβ is a well-known phenomenon in liver tumors, where the implication of caveolin is recently described [53]. When autocrine TGFβ production starts in tumor cells, it triggers EMT and contributes to the tumor invasion. Except for HuH7, decorin significantly reduced TGFβ levels in each hepatoma cell line. Since our studies were performed in a serum free environment, the TGFβ found in the

medium derived from tumor cells, however, we do not know whether the growth factor produced by the hepatomas became activated. It is certain that by reducing the TGFβ level, decorin may inhibit EMT and, if cells have already undergone EMT, it can hinder the tumor promoting activity of the cytokine.

In summary, our results demonstrate that the impact of decorin is highly cell-type specific reflecting on the reality of cancer biology. However, *in vitro* experiments have their limitations, e.g. unable to capture interactions between the tumor microenvironment and hepatoma cells, to extrapolate *in vitro* doses to *in vivo*, to detect the consequences, adverse effects of long-term treatment. To gain further insights to the molecular mechanisms behind antitumor actions of decorin, additional *in vivo* studies are needed.

5. Conclusions

Decorin proved to be an effective tumor suppressor on hepatocellular carcinoma cell lines *in vitro*. Proliferation rate of each cell line was hindered, although the least differentiated HLE showed only a modest reaction in MTT assays. All the cell lines responded to decorin exposure at molecular level, however they activated different signaling pathways according to their origin and differentiation state. Upon decorin exposure HepG2 followed the previously described canonical reactions, such as EGFR dephosphorlyation, and $p21^{WAF1/CIP1}$ activation, but other cell lines reacted differently. Decorin modulated the insulin receptor phosphorylation in Hep3B and HuH7 cells, which receptor was not described as an interacting partner of decorin before. We found G2/M phase cell cycle blockade in Hep3B, which is also a novel way how decorin exerts its antiproliferative effect. In HLE decorin action is accomplished via TGFβ1 pathway which seems to have weak influence on proliferation.

We can conclude that action of decorin highly depends on the molecular background of the hepatomas, despite the same tissue of origin or similar morphology.

List of abbreviations

BSA	bovine serum albumin
CDC25A	cell division cycle 25 homolog A
CDK	cyclin dependent kinase
DAPI	4′,6-diamidino-2-phenylindole
DCN	decorin
DEN	diethylnitrosamine
DMEM	Dulbecco's modified Eagle's medium
DMSO	dimethyil sulfoxide
ECM	extracellular matrix
EDTA	ethylenediaminetetraacetic acid
EGFR	epidermal growth factor receptor
ELISA	enzyme-linked immunosorbent assay
EMT	epithelial–mesenchymal transition
ErbB2	Receptor tyrosine-protein kinase erbB-2; erythroblastic oncogene B
ERK 1/2	extracellular signal-regulated kinase 1/2
FBS	fetal bovine serum
GAG	glycosaminoglycan

GSK3	glycogen synthase kinase 3
HCC	hepatocellular carcinoma
HGF	hepatocyte growth factor
IC	immunocytochemistry
IGF-IR	insulin-like growth factor 1 receptor
InsR	insulin receptor
IRS	Insulin receptor substrate
MAPK	mitogen-activated protein kinase
Met	hepatocyte growth factor receptor
MTT	3-(4,5-dimethylthiazol-2-yl)-2,5-diphenyltetrazolium bromide
PBS	phosphate buffered saline
PDGF	platelet-derived growth factor
PKB	protein kinase B
PVDF	polyvinylidene difluoride
Rb	retinoblastoma protein
RTK	receptor tyrosine kinase
SLRP	small leucine rich proteoglycan
TAA	thioacetamide
TBS	tris buffered saline

TGFb	transforming growth factor beta
TP53	p53 protein gene
VEGFR-2	vascular endothelial growth factor receptor 2
WB	Western blot
WNT	proto-oncogene protein Wnt

Declarations

Ethics approval and consent to participate

Not applicable

Consent for publication

Not applicable

Availability of data and material

The datasets used and/or analysed during the current study are available from the corresponding author on reasonable request.

Competing interests

Not applicable

Funding

The research work presented in the manuscript has been supported by the Hungarian National Research Fund „OTKA" number 105763 (to KB), 100904 and 119283 (to IK) and EU H2020 MSCA-RISE project #645756 GLYCANC.

Authors' contributions

ZH conducted the *in vitro* experiments and performed immunofluorescent and biochemical examinations. ZH and KB analyzed and interpreted the research data, and were major contributors in writing the manuscript. AR performed additional experiments, and helped in edition of figures. LS designed and provided the decorin expression vector. TD conducted short-term *in vitro* experiments, IK supervised the manuscript and finalized the background and discussion sections. All authors read and approved the final manuscript.

Acknowledgements

Not applicable

References

1. Ferlay, J., et al., *Cancer incidence and mortality worldwide: sources, methods and major patterns in GLOBOCAN 2012.* Int J Cancer, 2015. **136**(5): p. E359-86 DOI: 10.1002/ijc.29210.
2. Balogh, J., et al., *Hepatocellular carcinoma: a review.* J Hepatocell Carcinoma, 2016. **3**: p. 41-53 DOI: 10.2147/JHC.S61146.
3. Ramakrishna, G., et al., *From cirrhosis to hepatocellular carcinoma: new molecular insights on inflammation and cellular senescence.* Liver Cancer, 2013. **2**(3-4): p. 367-83 DOI: 10.1159/000343852.
4. Baghy, K., R.V. Iozzo, and I. Kovalszky, *Decorin-TGFbeta axis in hepatic fibrosis and cirrhosis.* J Histochem Cytochem, 2012. **60**(4): p. 262-8 DOI: 10.1369/0022155412438104.

5. Iozzo, R.V., *The family of the small leucine-rich proteoglycans: key regulators of matrix assembly and cellular growth.* Crit Rev Biochem Mol Biol, 1997. **32**(2): p. 141-74.
6. Dudas, J., et al., *Expression of decorin, transforming growth factor-beta 1, tissue inhibitor metalloproteinase 1 and 2, and type IV collagenases in chronic hepatitis.* Am J Clin Pathol, 2001. **115**(5): p. 725-35.
7. Baghy, K., et al., *Proteoglycans in liver cancer.* World J Gastroenterol, 2016. **22**(1): p. 379-93 DOI: 10.3748/wjg.v22.i1.379.
8. Santra, M., et al., *De novo decorin gene expression suppresses the malignant phenotype in human colon cancer cells.* Proc Natl Acad Sci U S A, 1995. **92**(15): p. 7016-20.
9. Nash, M.A., A.E. Loercher, and R.S. Freedman, *In vitro growth inhibition of ovarian cancer cells by decorin: synergism of action between decorin and carboplatin.* Cancer Res, 1999. **59**(24): p. 6192-6.
10. Araki, K., et al., *Decorin suppresses bone metastasis in a breast cancer cell line.* Oncology, 2009. **77**(2): p. 92-9 DOI: 10.1159/000228253.
11. Grant, D.S., et al., *Decorin suppresses tumor cell-mediated angiogenesis.* Oncogene, 2002. **21**(31): p. 4765-77.
12. Reed, C.C., et al., *Decorin prevents metastatic spreading of breast cancer.* Oncogene, 2005. **24**(6): p. 1104-10.
13. Koninger, J., et al., *Overexpressed decorin in pancreatic cancer: potential tumor growth inhibition and attenuation of chemotherapeutic action.* Clin Cancer Res, 2004. **10**(14): p. 4776-83 DOI: 10.1158/1078-0432.CCR-1190-03.
14. Skandalis, S.S., et al., *The increased accumulation of structurally modified versican and decorin is related with the progression of laryngeal cancer.* Biochimie, 2006. **88**(9): p. 1135-43 DOI: 10.1016/j.biochi.2006.03.011.
15. Zhang, Y., et al., *Recombinant human decorin suppresses liver HepG2 carcinoma cells by p21 upregulation.* Onco Targets Ther, 2012. **5**: p. 143-52 DOI: 10.2147/OTT.S32918.
16. Horvath, Z., et al., *Decorin deficiency promotes hepatic carcinogenesis.* Matrix Biol, 2014. **35**: p. 194-205 DOI: 10.1016/j.matbio.2013.11.004.
17. Iozzo, R.V., et al., *Decorin is a biological ligand for the epidermal growth factor receptor.* J Biol Chem, 1999. **274**(8): p. 4489-92.
18. Schonherr, E., et al., *Decorin, a novel player in the insulin-like growth factor system.* J Biol Chem, 2005. **280**(16): p. 15767-72.

19. Santra, M., I. Eichstetter, and R.V. Iozzo, *An anti-oncogenic role for decorin. Down-regulation of ErbB2 leads to growth suppression and cytodifferentiation of mammary carcinoma cells.* J Biol Chem, 2000. **275**(45): p. 35153-61.
20. Goldoni, S., et al., *Decorin is a novel antagonistic ligand of the Met receptor.* J Cell Biol, 2009. **185**(4): p. 743-54.
21. Khan, G.A., et al., *Decorin is a novel VEGFR-2-binding antagonist for the human extravillous trophoblast.* Mol Endocrinol, 2011. **25**(8): p. 1431-43 DOI: 10.1210/me.2010-0426.
22. Baghy, K., et al., *Decorin interferes with platelet-derived growth factor receptor signaling in experimental hepatocarcinogenesis.* Febs Journal, 2013. **280**(10): p. 2150-2164 DOI: 10.1111/febs.12215.
23. Yamaguchi, Y., D.M. Mann, and E. Ruoslahti, *Negative regulation of transforming growth factor-beta by the proteoglycan decorin.* Nature, 1990. **346**(6281): p. 281-4.
24. Morrione, A., T. Neill, and R.V. Iozzo, *Dichotomy of decorin activity on the insulin-like growth factor-I system.* FEBS J, 2013. **280**(10): p. 2138-49 DOI: 10.1111/febs.12149.
25. Neill, T., L. Schaefer, and R.V. Iozzo, *Decorin as a multivalent therapeutic agent against cancer.* Adv Drug Deliv Rev, 2016. **97**: p. 174-85 DOI: 10.1016/j.addr.2015.10.016.
26. Sofeu Feugaing, D.D., M. Gotte, and M. Viola, *More than matrix: the multifaceted role of decorin in cancer.* Eur J Cell Biol, 2013. **92**(1): p. 1-11 DOI: 10.1016/j.ejcb.2012.08.004.
27. Neill, T., L. Schaefer, and R.V. Iozzo, *Decorin: a guardian from the matrix.* Am J Pathol, 2012. **181**(2): p. 380-7 DOI: 10.1016/j.ajpath.2012.04.029.
28. McBain, A.L. and D.M. Mann, *Purification of recombinant human decorin and its subdomains.* Methods Mol Biol, 2001. **171**: p. 221-9 DOI: 10.1385/1-59259-209-0:221.
29. Davis, G.L., et al., *Hepatocellular carcinoma: management of an increasingly common problem.* Proc (Bayl Univ Med Cent), 2008. **21**(3): p. 266-80.
30. Hamid, A.S., et al., *Recombinant human decorin upregulates p57KIP(2) expression in HepG2 hepatoma cell lines.* Mol Med Rep, 2013. **8**(2): p. 511-6 DOI: 10.3892/mmr.2013.1510.
31. Santra, M., C.C. Reed, and R.V. Iozzo, *Decorin binds to a narrow region of the epidermal growth factor (EGF) receptor, partially overlapping but distinct from the EGF-binding epitope.* J Biol Chem, 2002. **277**(38): p. 35671-81.

32. Ding, Q., et al., *Erk associates with and primes GSK-3beta for its inactivation resulting in upregulation of beta-catenin.* Mol Cell, 2005. **19**(2): p. 159-70 DOI: 10.1016/j.molcel.2005.06.009.
33. Wu, D. and W. Pan, *GSK3: a multifaceted kinase in Wnt signaling.* Trends Biochem Sci, 2010. **35**(3): p. 161-8 DOI: 10.1016/j.tibs.2009.10.002.
34. Soussi, T. and K.G. Wiman, *TP53: an oncogene in disguise.* Cell Death Differ, 2015. **22**(8): p. 1239-49 DOI: 10.1038/cdd.2015.53.
35. Liu, J., et al., *Tumor suppressor p53 and its mutants in cancer metabolism.* Cancer Lett, 2015. **356**(2 Pt A): p. 197-203 DOI: 10.1016/j.canlet.2013.12.025.
36. Kung, C.P. and M.E. Murphy, *The role of the p53 tumor suppressor in metabolism and diabetes.* J Endocrinol, 2016. **231**(2): p. R61-R75 DOI: 10.1530/JOE-16-0324.
37. Werner, H., et al., *Insulin-like Growth Factor 1 Signaling Axis Meets p53 Genome Protection Pathways.* Front Oncol, 2016. **6**: p. 159 DOI: 10.3389/fonc.2016.00159.
38. Boissan, M., et al., *Overexpression of insulin receptor substrate-2 in human and murine hepatocellular carcinoma.* Am J Pathol, 2005. **167**(3): p. 869-77 DOI: 10.1016/S0002-9440(10)62058-5.
39. Xiong, L., et al., *A novel role for IGF-1R in p53-mediated apoptosis through translational modulation of the p53-Mdm2 feedback loop.* J Cell Biol, 2007. **178**(6): p. 995-1007 DOI: 10.1083/jcb.200703044.
40. Yoon, A.R., J. Hong, and C.O. Yun, *Adenovirus-mediated decorin expression induces cancer cell death through activation of p53 and mitochondrial apoptosis.* Oncotarget, 2017. **8**(44): p. 76666-76685 DOI: 10.18632/oncotarget.20800.
41. Mitry, R.R., et al., *Wild-type p53 induces apoptosis in Hep3B through up-regulation of bax expression.* Lab Invest, 1997. **77**(4): p. 369-78.
42. Benada, J. and L. Macurek, *Targeting the Checkpoint to Kill Cancer Cells.* Biomolecules, 2015. **5**(3): p. 1912-37 DOI: 10.3390/biom5031912.
43. Miller, D.M., et al., *c-Myc and cancer metabolism.* Clin Cancer Res, 2012. **18**(20): p. 5546-53 DOI: 10.1158/1078-0432.CCR-12-0977.
44. Guegan, J.P., et al., *MAPK signaling in cisplatin-induced death: predominant role of ERK1 over ERK2 in human hepatocellular carcinoma cells.* Carcinogenesis, 2013. **34**(1): p. 38-47 DOI: 10.1093/carcin/bgs317.
45. Sheridan, C., et al., *An ERK-dependent pathway to Noxa expression regulates apoptosis by platinum-based chemotherapeutic drugs.* Oncogene, 2010. **29**(49): p. 6428-41 DOI: 10.1038/onc.2010.380.

46. Tsukada, Y., K. Miyazawa, and N. Kitamura, *High intensity ERK signal mediates hepatocyte growth factor-induced proliferation inhibition of the human hepatocellular carcinoma cell line HepG2.* J Biol Chem, 2001. **276**(44): p. 40968-76 DOI: 10.1074/jbc.M010890200.

47. Dor, I., M. Namba, and J. Sato, *Establishment and some biological characteristics of human hepatoma cell lines.* Gan, 1975. **66**(4): p. 385-92.

48. Xu, W., Z. Yang, and N. Lu, *A new role for the PI3K/Akt signaling pathway in the epithelial-mesenchymal transition.* Cell Adh Migr, 2015. **9**(4): p. 317-24 DOI: 10.1080/19336918.2015.1016686.

49. Lee, T.K., et al., *CD24(+) liver tumor-initiating cells drive self-renewal and tumor initiation through STAT3-mediated NANOG regulation.* Cell Stem Cell, 2011. **9**(1): p. 50-63 DOI: 10.1016/j.stem.2011.06.005.

50. Hausser, H., O. Witt, and H. Kresse, *Influence of membrane-associated heparan sulfate on the internalization of the small proteoglycan decorin.* Exp Cell Res, 1993. **208**(2): p. 398-406 DOI: 10.1006/excr.1993.1261.

51. Schaefer, L., et al., *Decorin, biglycan and their endocytosis receptor in rat renal cortex.* Kidney Int, 1998. **54**(5): p. 1529-41 DOI: 10.1046/j.1523-1755.1998.00149.x.

52. Dituri, F., et al., *Differential Inhibition of the TGF-beta Signaling Pathway in HCC Cells Using the Small Molecule Inhibitor LY2157299 and the D10 Monoclonal Antibody against TGF-beta Receptor Type II.* PLoS One, 2013. **8**(6): p. e67109 DOI: 10.1371/journal.pone.0067109.

53. Moreno-Caceres, J., et al., *The level of caveolin-1 expression determines response to TGF-beta as a tumour suppressor in hepatocellular carcinoma cells.* Cell Death Dis, 2017. **8**(10): p. e3098 DOI: 10.1038/cddis.2017.469.

Legends to Figures

Figure 1. Proliferation rate of hepatoma cell lines after decorin treatment. (DCN100 = 100 μg/ml decorin in cell culture media) compared and normalized to control cells. Data are expressed as mean of normalized values±SD. *p<0.05; ** p<0.01; *** p<0.001.

Figure 2. TGF-β1 production of HepG2, Hep3B, HuH7 and HLE hepatoma cell lines exposed to decorin. Diagram shows normalized TGF-β1 levels after 48 h of decorin treatment from media of hepatoma cell lines. *p<0.05; ** p<0.01.

Figure 3. Activity of receptor tyrosine kinases in HepG2, Hep3B and HuH7 cell lines after 48h of decorin treatment. Bar charts show the levels of detected phospho-receptors in decorin treated groups compared to the untreated controls in each cell line *p<0.05; ** p<0.01; *** p<0.001.

Figure 4. Western blot analysis of various signaling proteins in HepG2 cells after 48h of decorin treatment. Beta-actin was used as loading control (A). Bar charts represent the relative amount of investigated proteins in DCN50 and DCN100 treated cells (B). Data are shown as mean of normalized values±SD. *p<0.05; ** p<0.01; *** p<0.001.

Figure 5. Representative images of immunocytochemical analysis of β-catenin localization in control (A) and decorin treated (B) HepG2 cells, as well as in control HLE cells (C) and after decorin exposure (F). Scale bar =10 μm (A, B) and 50 μm (C, D).

Figure 6. Western blot analysis of various signaling proteins in HepB3 cells after 48h of decorin treatment. Beta-actin was used as loading control (A). Bar charts represent the relative amount of investigated proteins in DCN50 and DCN100 treated cells (B). Data are shown as mean of normalized values±SD. *p<0.05; ** p<0.01; *** p<0.001.

Figure 7. Analysis of CDK1 regulation in Hep3B hepatoma cell line after 48h of decorin treatment. (A) Representative Western blots of phospho-CDK1 protein levels in DCN50 and DCN100 treated cells (A). Bar charts represent the relative values of detected pCDK1 signals (B). Beta-actin was used as loading control. Real-time PCR analysis of CDC25A (C) and Wee1(D) mRNA levels in the same experiment. Data are shown as mean of normalized values±SD.** p<0.01.

Figure 8. Western blot analysis of various signaling proteins in HuH7 cells after 48h of decorin treatment. Beta-actin was used as loading control (A). Bar charts represent the relative amount of investigated proteins in DCN50 and DCN100 treated cells (B). Data are shown as mean of normalized values±SD. *p<0.05; ** p<0.01; *** p<0.001.

Figure 9. Western blot analysis of various signaling proteins in HLE cells after 48h of decorin treatment. Beta-actin was used as loading control (A). Bar charts represent the relative amount of investigated proteins in DCN50 and DCN100 treated cells (B). Data are shown as mean of normalized values±SD. *p<0.05; ** p<0.01; *** p<0.001.

Figure 10. Schematic illustration of signaling pathways affected by decorin exposure in HepG2, Hep3B, HuH7 and HLE cell lines. Green color indicates molecules with altered level

or activity. The direction of change is marked by arrows. Blue color indicates proteins with levels unchanged. Grey color indicates molecules not examined in our experiments.

Figure S1. Activity of receptor tyrosine kinases in HepG2, Hep3B and HuH7 cell lines after 15 min of decorin treatment.

Figure 1.

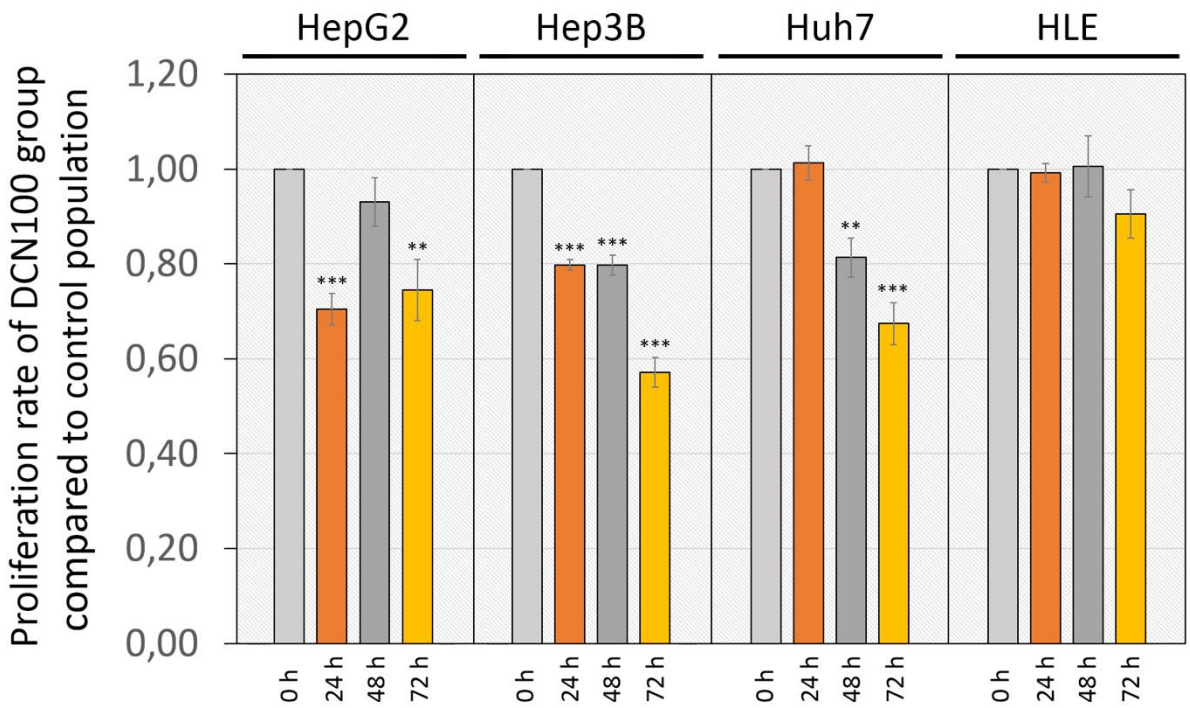
HepG2
Hep3B
Huh7
HLE
Proliferation rate of DCN100 group compared to control population
1,20
1,00
0,80
0,60
0,40
0,20
0,00
***
**
***
***
***
**
***
0 h
24 h
48 h
72 h

Figure 2.

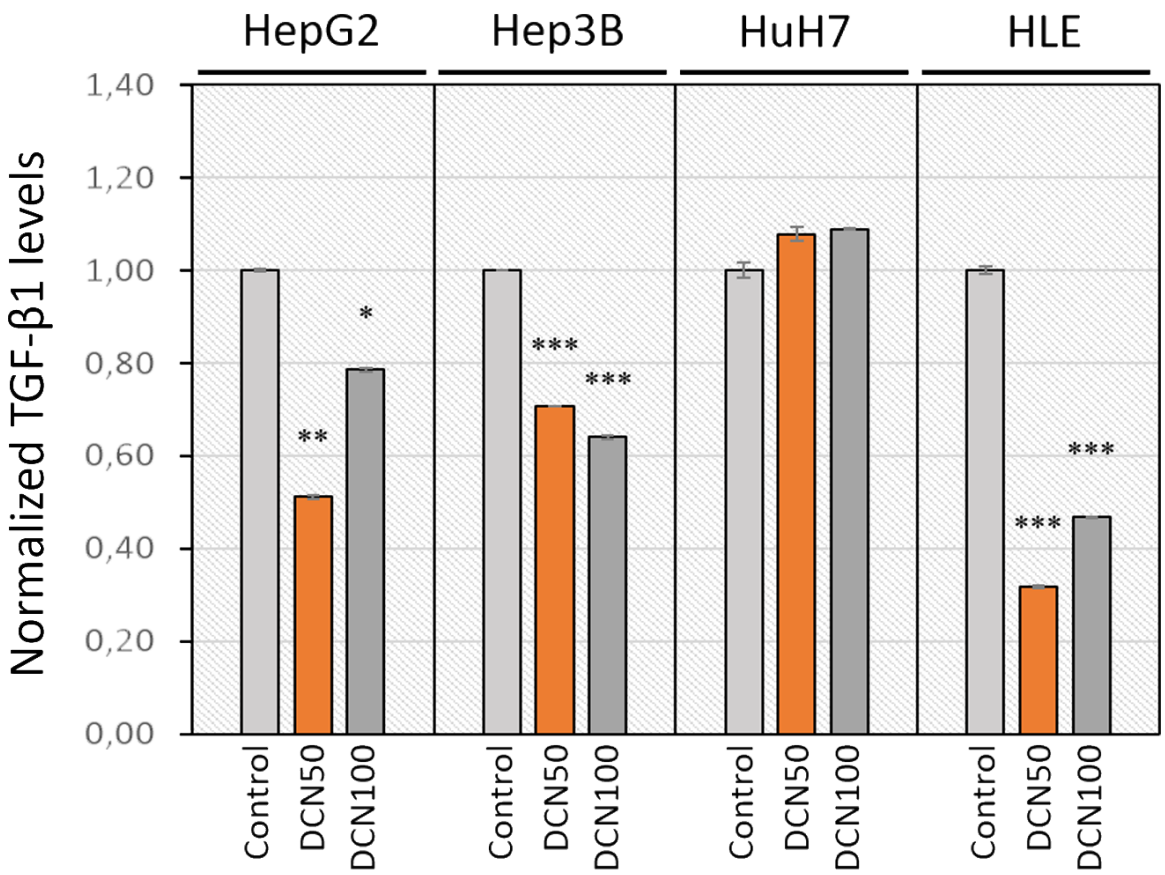
HepG2
Hep3B
HuH7
HLE
Normalized TGF-β1 levels
1,40
1,20
1,00
0,80
0,60
0,40
0,20
0,00
**
*
***
***
***
***
Control
DCN50
DCN100
Control
DCN50
DCN100
Control
DCN50
DCN100
Control
DCN50
DCN100

Figure 3.

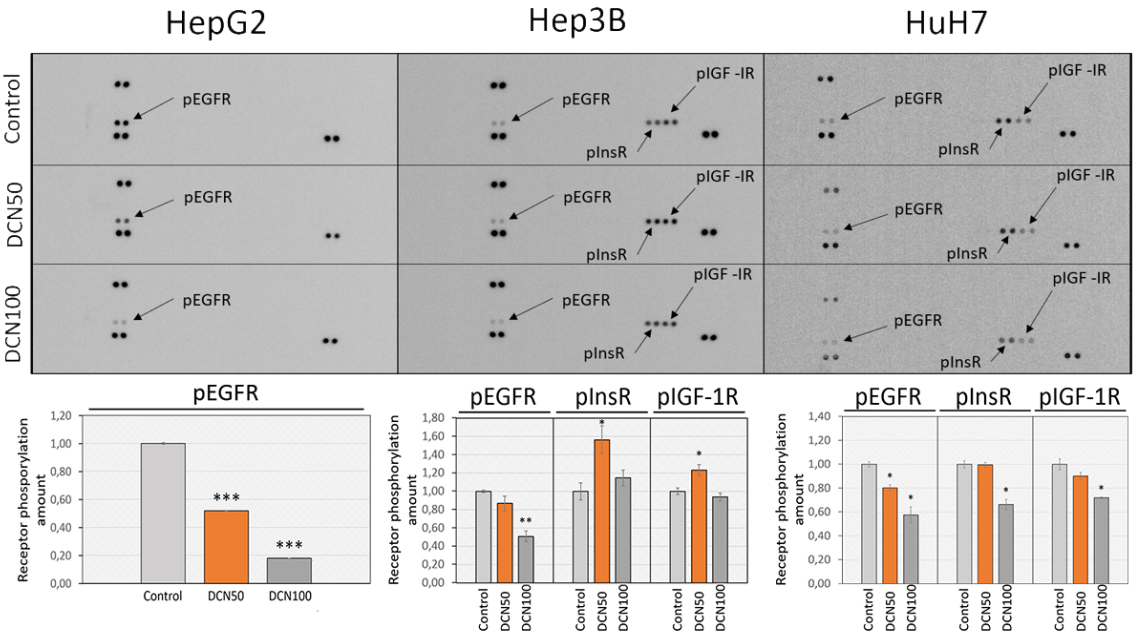
HepG2
Hep3B
HuH7
Control
DCN50
DCN100
pEGFR
pIGF -IR
pInsR
pEGFR
pInsR
pIGF-1R
Receptor phosphorylation amount
Control
DCN50
DCN100

Figure 4.

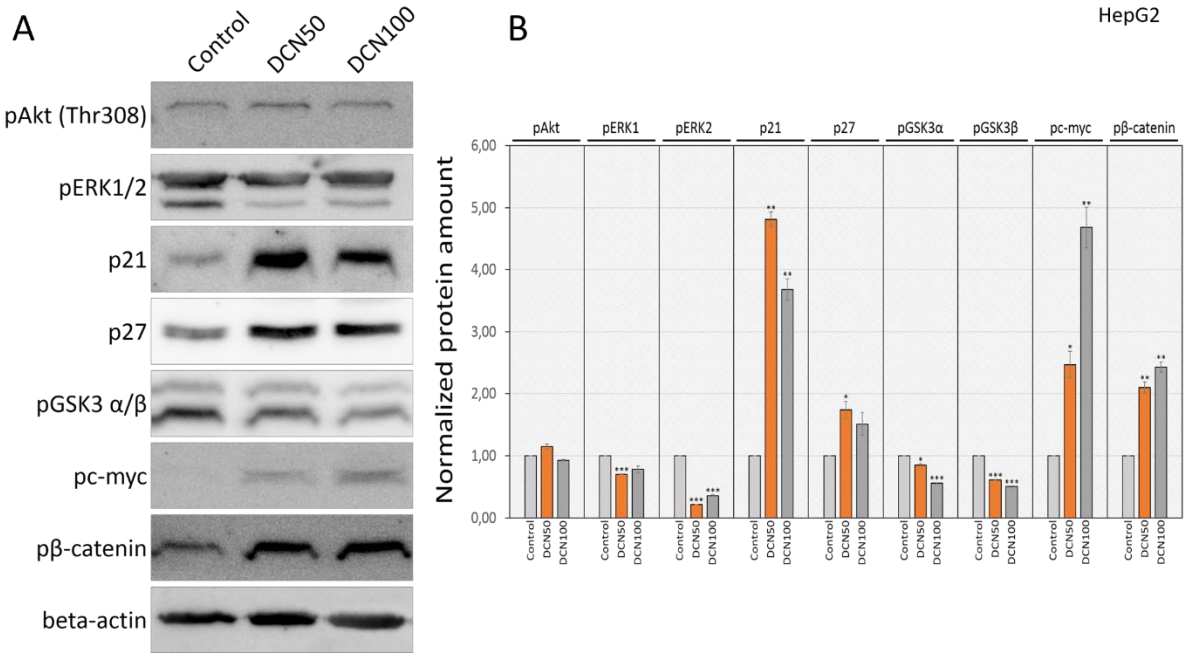
A
Control
DCN50
DCN100
pAkt (Thr308)
pERK1/2
p21
p27
pGSK3 α/β
pc-myc
pβ-catenin
beta-actin
B
HepG2
Normalized protein amount
pAkt
pERK1
pERK2
p21
p27
pGSK3α
pGSK3β
pc-myc
pβ-catenin
6,00
5,00
4,00
3,00
2,00
1,00
0,00
Control
DCN50
DCN100

Figure 5.

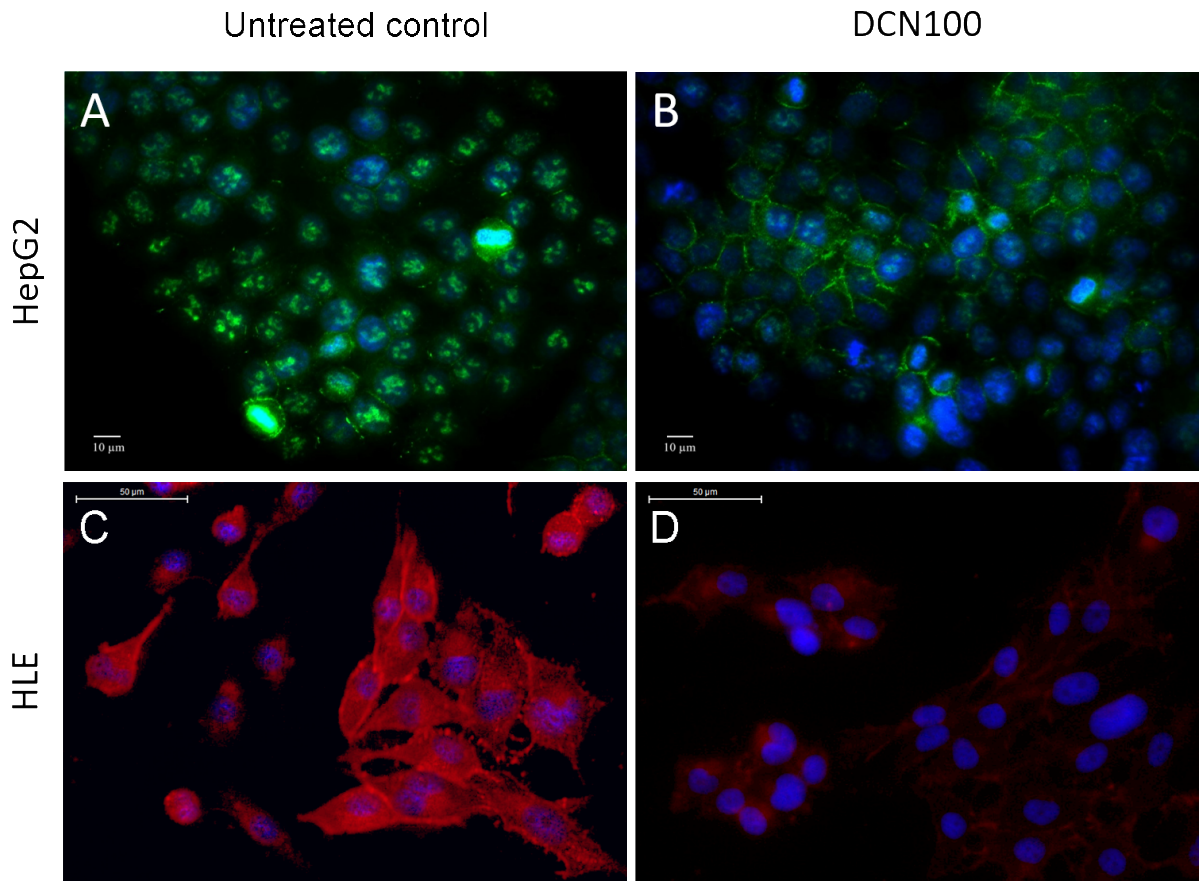
Untreated control
DCN100
HepG2
HLE
A
B
C
D
10 µm
10 µm
50 µm
50 µm

Figure 6.

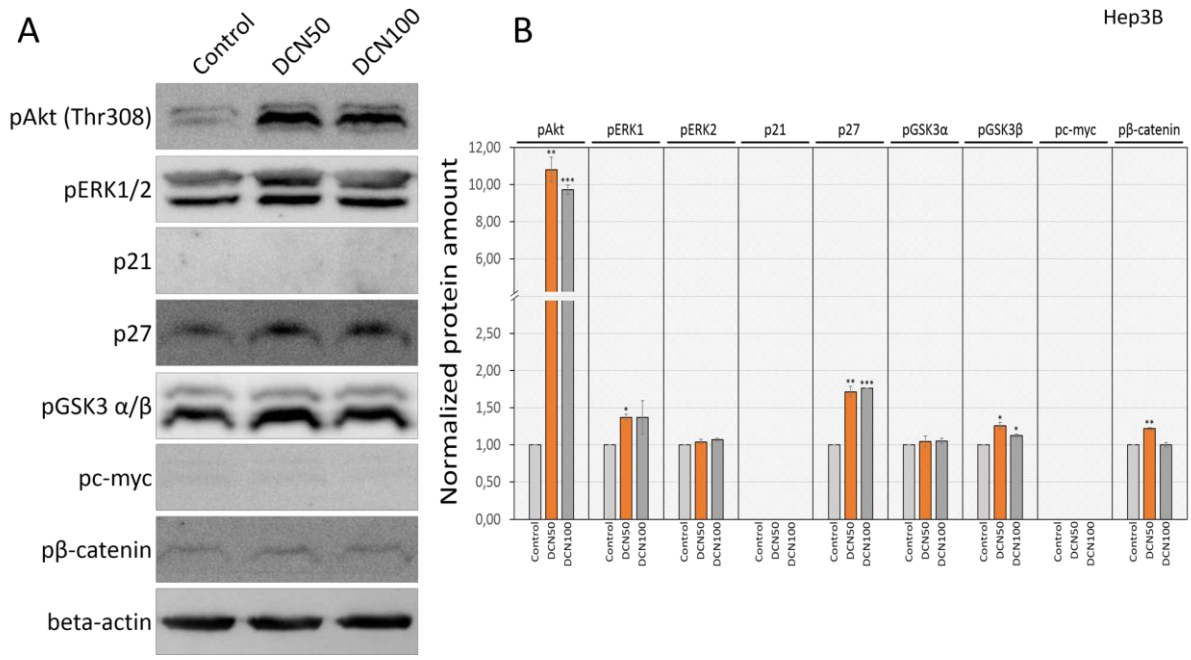
A
Control
DCN50
DCN100
pAkt (Thr308)
pERK1/2
p21
p27
pGSK3 α/β
pc-myc
pβ-catenin
beta-actin
B
Hep3B
Normalized protein amount
pAkt
pERK1
pERK2
p21
p27
pGSK3α
pGSK3β
pc-myc
pβ-catenin
12,00
10,00
8,00
6,00
2,50
2,00
1,50
1,00
0,50
0,00
Control
DCN50
DCN100

Figure 7.

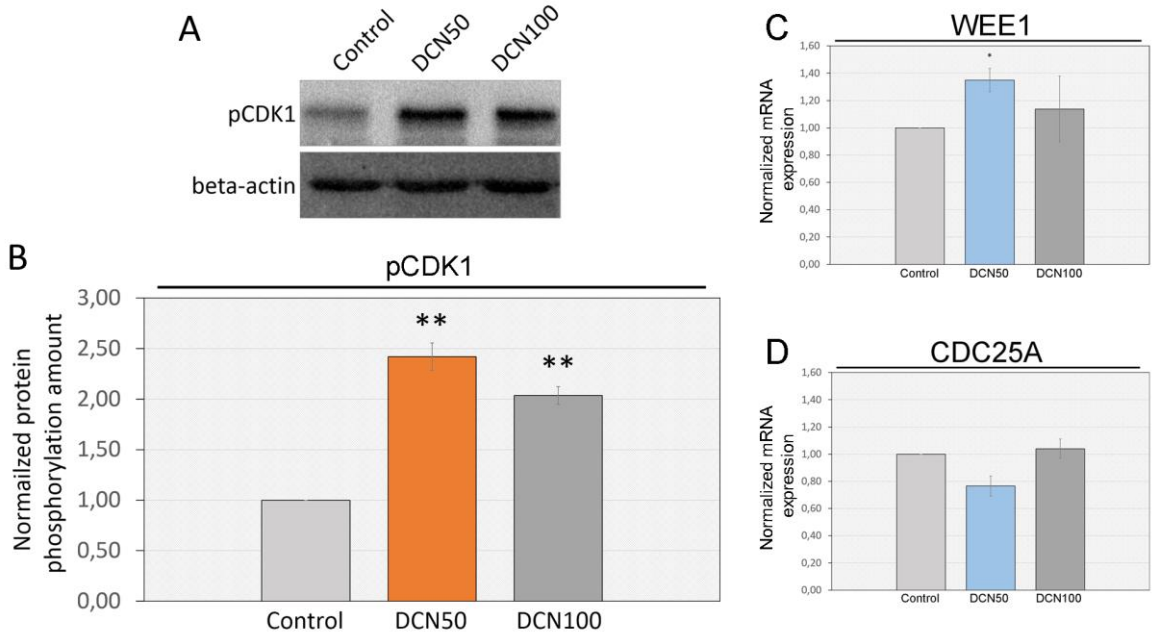
A
Control
DCN50
DCN100
pCDK1
beta-actin
B
pCDK1
Normailzed protein phosphorylation amount
3,00
2,50
2,00
1,50
1,00
0,50
0,00
**
**
Control
DCN50
DCN100
C
WEE1
Normalized mRNA expression
1,60
1,40
1,20
1,00
0,80
0,60
0,40
0,20
0,00
Control
DCN50
DCN100
D
CDC25A
Normalized mRNA expression
1,60
1,40
1,20
1,00
0,80
0,60
0,40
0,20
0,00
Control
DCN50
DCN100

Figure 8.

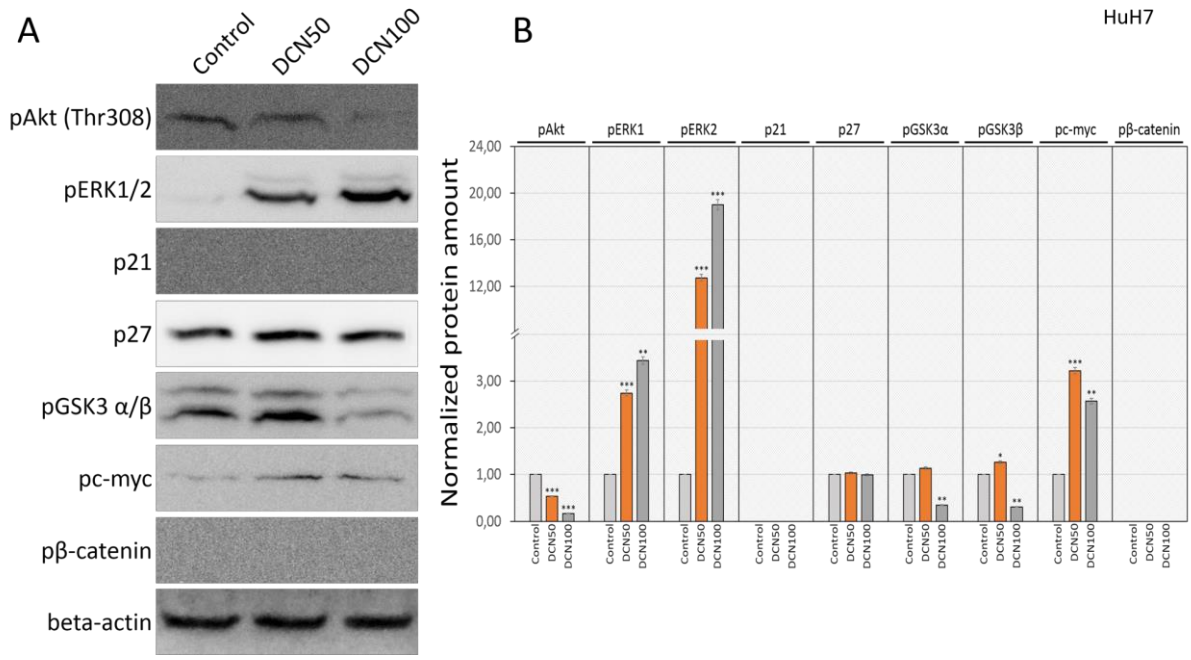
A
Control
DCN50
DCN100
pAkt (Thr308)
pERK1/2
p21
p27
pGSK3 α/β
pc-myc
pβ-catenin
beta-actin
B
HuH7
pAkt
pERK1
pERK2
p21
p27
pGSK3α
pGSK3β
pc-myc
pβ-catenin
Normalized protein amount
24,00
20,00
16,00
12,00
3,00
2,00
1,00
0,00
Control
DCN50
DCN100

Figure 9.

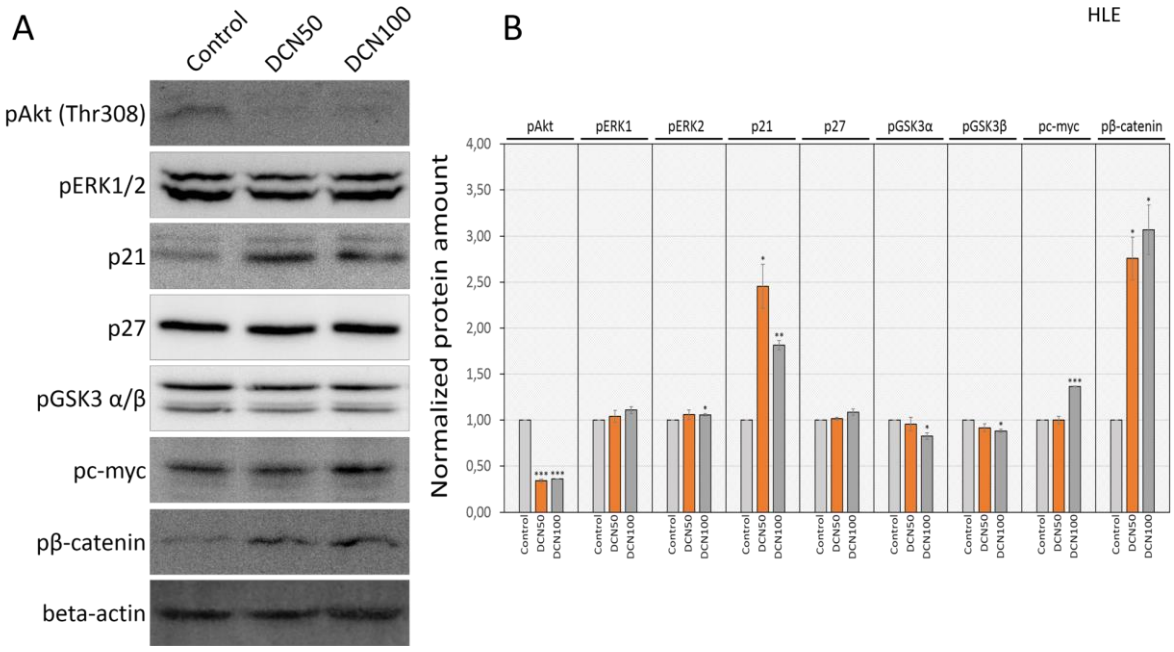
A
Control
DCN50
DCN100
pAkt (Thr308)
pERK1/2
p21
p27
pGSK3 α/β
pc-myc
pβ-catenin
beta-actin
B
HLE
Normalized protein amount
pAkt
pERK1
pERK2
p21
p27
pGSK3α
pGSK3β
pc-myc
pβ-catenin
4,00
3,50
3,00
2,50
2,00
1,50
1,00
0,50
0,00
Control
DCN50
DCN100

Figure 10.

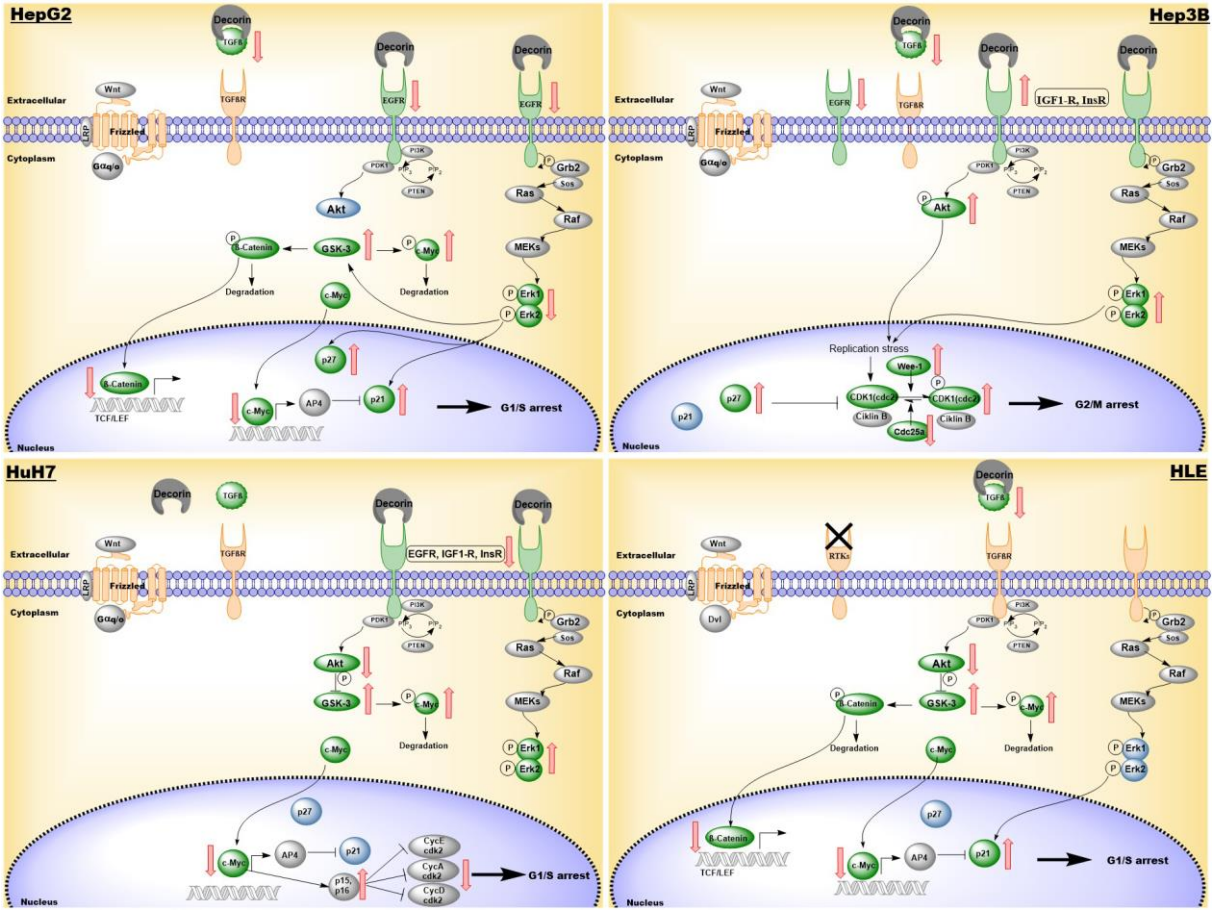
HepG2
Hep3B
HuH7
HLE
Extracellular
Cytoplasm
Nucleus
Decorin
TGFβ
TGFβR
Wnt
Frizzled
LRP
Gαq/o
EGFR
PI3K
PDK1
PIP3
PIP2
PTEN
Grb2
Sos
Ras
Raf
MEKs
Erk1
Erk2
Akt
GSK-3
β-Catenin
c-Myc
Degradation
TCF/LEF
p27
AP4
p21
G1/S arrest
IGF1-R, InsR
Replication stress
Wee-1
CDK1(cdc2)
Ciklin B
Cdc25a
G2/M arrest
EGFR, IGF1-R, InsR
CycE cdk2
CycA cdk2
CycD cdk2
p15, p16
RTKs
Dvl

Figure S1

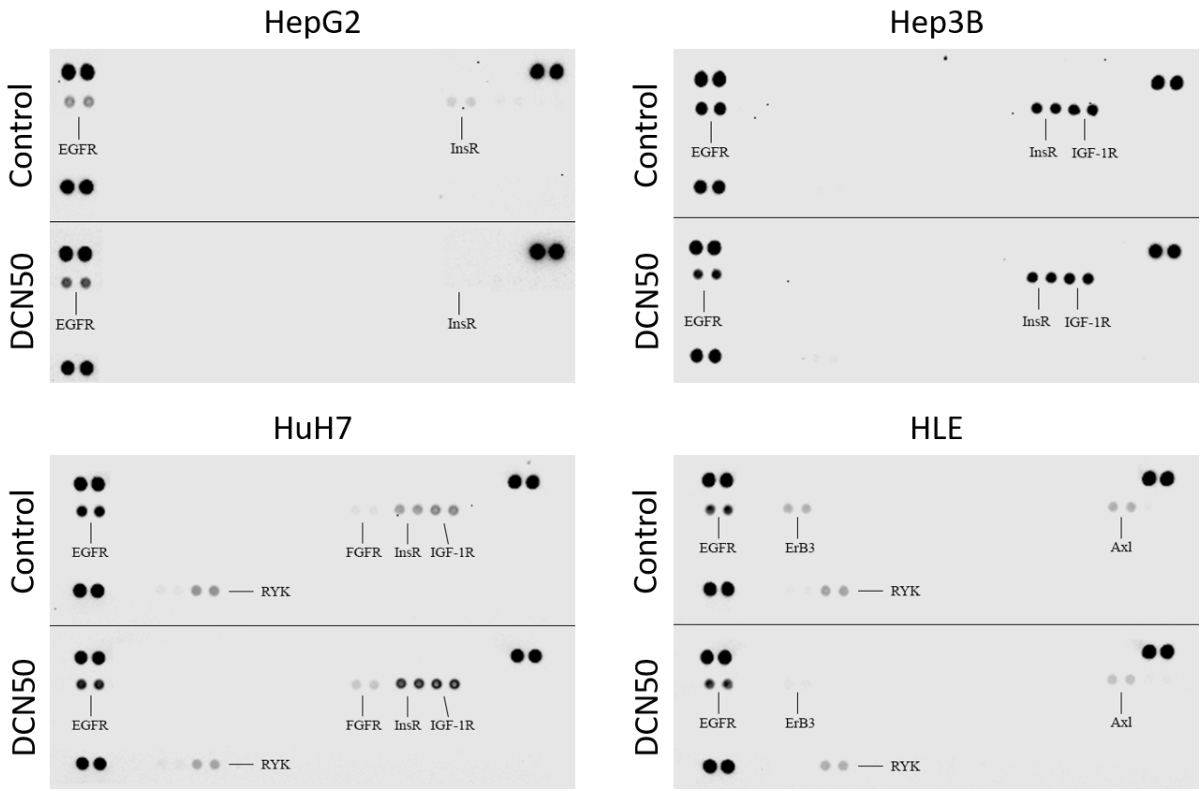
HepG2
Control
EGFR
InsR
DCN50
EGFR
InsR
Hep3B
Control
EGFR
InsR
IGF-1R
DCN50
EGFR
InsR
IGF-1R
HuH7
Control
EGFR
FGFR
InsR
IGF-1R
RYK
DCN50
EGFR
FGFR
InsR
IGF-1R
RYK
HLE
Control
EGFR
ErB3
Axl
RYK
DCN50
EGFR
ErB3
Axl
RYK

Supplementary Table 1. Antibodies used in the present study.

Antigen	Species	Manufacturer*	Cat. No	Dilution for WB	Dilution for IC
β-Catenin	Rabbit polyclonal	Atlas Antibodies	HPA029159	-	1:100
Phospho-β-Catenin (Ser33/34/Thr41)	Rabbit polyclonal	Cell Signaling	9561	1:1000	-
Phospho-c-Myc (Thr58)	Rabbit polyclonal	Thermo Fisher	PA1-14268	1:1000	-
Phospho-p44/42 MAP Kinase (Thr202/204)	Rabbit monoclonal	Cell Signaling	4370	1:1000	-
$p21^{Waf1/Cip1}$	Rabbit polyclonal	Abcam	ab7960	1:200	-
β-actin	Mouse monoclonal	Sigma	A2228	1:5000	-
phospho-CDK1	Rabbit polyclonal	Novus (R&D)	nbp1-19966	1:500	-
$p27^{Kip1}$	Mouse monoclonal	Thermo Fisher	AHZ0458	1:1000	-
Phospho-Akt (Thr308)	Rabbit monoclonal	Cell Signaling	2965	1:500	-
Phospho GSK3α/β (Ser21/9)	Rabbit polyclonal	Cell Signaling	9331	1:1000	-
Secondary antibodies	**Species**	**Manufacturer***	**Catalog number**	**Dilution for WB**	**Dilution for IC**
Anti-rabbit immunoglobulins/HRP	Goat polyclonal	DakoCytomation	P 0448	1:2000	-
Anti-goat immunoglobulins/HRP	Rabbit polyclonal	DakoCytomation	P 0449	1:2000	-
Anti-rabbit immunoglobulins/biotin	Goat polyclonal	DakoCytomation	E 0432	-	1:200
Alexa Fluor 488 anti-goat IgG	Donkey	Invitrogen	A-11055	-	1:200
Alexa Fluor 555 anti-rabbit IgG	Donkey	Invitrogen	A-31572	-	1:200

* R&D Systems Minneapolis, MN, DakoCytomation Glostrup Denmark, Invitrogen/Life Technologies Carlsbad CA, Abcam Cambrige UK, Cell Signaling Technology Danvers, MA, Abnova Taipei Taiwan, Thermo Fischer Rockfort IL, Atlas Antibodies Stockholm Sweden, Sigma-Aldrich St. Louis, MO, Calbiochem/Millipore Billerica MA.